Molecular dynamics study of crystallization of polymer systems confined in small nanodomains

Toshiaki Miura and Masuhiro Mikami
National Institute of Advanced Industrial Science and Technology (AIST) AIST Central2, 1-1 Umezono, Tsukuba, Ibaraki 305-8568, Japan

(Received 21 July 2006; revised manuscript received 1 December 2006; published 29 March 2007)

We study the ordering dynamics of polymer crystallization using molecular dynamics simulations, in which the polymers are confined to small nanodomains surrounded by a noncrystalline medium. Although the adsorption process and surface diffusion of polymer chains play a major role in the case of the crystalline interface, the domain interface which consists of noncrystalline medium does not have such a crystal substrate to induce the growth of a crystal layer, which may lead to different ordering dynamics. We found that existence of a noncrystalline domain interface has two opposite effects. In the case of semiflexible polymer systems, the domain interface accelerates crystallization in the initial period, whereas it suppresses crystallization in the intermediate or late period. When the rigidity of polymer chains increases, the acceleration effect of the initial crystallization induced by the domain interface is sometimes hidden by spontaneous homogeneous nucleation. These ordering behaviors can be explained by the restriction on the local chain direction near the domain surface in the crystal nucleation stage and the restriction of large orientation relaxation and coalescence in the crystal growth stage. Simulation results reveal that the confinement by the noncrystalline medium does not have a simple effect on the polymer crystallization dynamics, but has various conflicting effects combined with the time stage, the rigidity of polymer chains, and the strength of the surrounding domain interface.

DOI: 10.1103/PhysRevE.75.031804 PACS number(s): 61.41.+e, 81.10.Aj

I. INTRODUCTION

In recent years, the crystallization of polymers in a small nanospace has been studied experimentally, mainly using crystalline-noncrystalline block copolymer systems [1–8]. There are characteristic behaviors and properties in the crystallization processes of the system confined to the nanodomain, which are different from those of the crystallization in the bulk polymers. Although the crystallinity, the orientation of chains, the crystallization temperature, and the ordering dynamics have been examined experimentally in various polymer systems, there remain many unresolved problems since crystallization is a complicated ordering process in which various factors are jointly concerned. For example, when we compare the crystallization in the microdomain with that in the bulk, it is very difficult to maintain the condition of impurities experimentally. Hence, it is considered that homogeneous nucleation dynamics is dominant in the nanodomain samples, whereas heterogeneous nucleation dynamics prevails in the case of bulk samples due to possible impurities in the system. The cause of the lower crystallization temperature in the nanodomains has been ascribed to this effect. However, since the amount of impurities cannot be controlled experimentally, discussions on these have to depend on indirect evidence. In addition, one might consider the additional constraint in the block copolymer cases. The junctions of the crystalline block and the noncrystalline block of polymer chains would exist in the domain interface region. Thus, it has been difficult to estimate the role and effect of various factors individually and obtain systematic knowledge for the ordering mechanism.

For the study of these complicated phenomena, molecular simulation is a useful tool. However, the precise reproduction of the experimental results by simulation using the full atomistic model is not always easy, mainly owing to the limitation of computational time and resources. In the case of these kinds of problems, coarse-grained models, which simplified unnecessary degrees of freedom and detailed structures, are useful for examining the basic mechanism of the ordering dynamics. Recently, molecular simulations of the crystallization have been applied to the system of dense polymer melts [9–24]. In these studies, the simulations of the polymer crystallization in the bulk have been carried out by imposing the periodic boundary condition. These simulation results showed the unique ordering behaviors that originate in the large internal degrees of freedom of polymers. In the meantime, simulations of polymer crystallization on the surface have been attempted mainly on the system of a planar crystalline interface, in which the dynamics of the growth of a crystal layer on this planar crystal substrate is the main subject of interest [16]. In this case, the principal processes required to control the ordering dynamics are the adsorption to the crystal substrate and the reorientation of the polymer chain on this crystalline surface, which are closely related to the secondary nucleation in the polymer crystallization. Quite recently, a Monte Carlo study on the crystallization of block copolymers that are two-dimensionally confined in cylindrical shape has been reported [24]. This study would give valuable information about the role of block junctions on chain orientation inside domains. However, detailed ordering dynamics, especially the difference between crystallization in the bulk, is still an unsettled question. Hence, the simulation of crystallization dynamics of dense polymer melts confined to three-dimensional nanodomains, in which the domain interface consists of the amorphous surface with no regular crystal structure, has not been systematically investigated until now.

It is worth noting that the studies of polymers confined to walls or thin films have been explored mainly on the configuration or thermal properties of polymer chains in the solution or melt [25–30]. As consequences, these systems are

often in the liquid states and well above the crystallization temperature if it exists. In these liquid simulations, the boundary conditions are mainly the confinement between two planes or thin free surface layer. Under such confinement, these polymer systems show features that differ from those of bulk systems, especially when the layer thickness is smaller than the radius of gyration of polymer chains. Although these results give us some insight on polymer behaviors in some kinds of small confined spaces, they are not always directly applicable to the crystallization problems in nanodomains. In the case of polymer crystallization in nanodomains, the size of a domain is not necessarily much smaller than the radius of gyration of polymer chains. The domain structure is usually formed by self-assembly and no forces compress the chains in a specific direction beyond the equilibrium distribution size of the chain. Therefore, the simulation results of the polymer configurations in liquid thin layers are not necessarily related to the ordering dynamics of polymer crystallization in nanodomains. In the case of polymer crystallization in nanodomains, it is not clear whether the dynamics of ordering processes might differ between a system confined to a crystalline interface and a system confined to a noncrystalline interface. This is because in the case of the crystalline interface, chain adsorption to the interface and reorientation by slip diffusion on the surface may play an important role, whereas in the case of the noncrystalline interface, there would be no explicit driving force to attract and align polymer chains on the domain surface. In addition, it may be interesting to investigate the effect of boundary shape, such as cubic geometry or spherical geometry, on the crystallization dynamics. Hence, in this study, we carried out molecular simulations of polymer crystallization both in the bulk and in nanodomains, and considered the effect of the noncrystalline interface on the ordering dynamics.

II. MODEL

We performed coarse-grained molecular dynamics simulations. Polymers are represented by the beads-springs model, in which the connectivity and bending rigidity of polymer chains are considered [9–11]. This polymer model is simpler than the united atom polymer model, which is often used for the simulation of alkane chain molecules. The segment unit of the coarse-grained model does not necessarily correspond to one carbon atom of a main chain. The segment sometimes corresponds to a group of carbon atoms in the united atom model, as in the case of theories of polymer dynamics in solutions and melts. The advantage of the coarse-grained model is the ease of crystallization and fast ordering dynamics. In the case of the united atom model, the rotational energy barriers slow down the chain dynamics significantly, which results in large amounts of calculations for the ordering processes. For the study of basic mechanisms in the ordering dynamics of polymer systems, simpler models that neglect inessential modes would be effective in elucidating the universal features and underlying physics of the complicated ordering processes.

In our coarse-grained model, the chain connectivity is introduced by standard harmonic potentials between the nearest-neighbor segments of the same main chains, as given by $U(b)=\frac{1}{2}K_0(b-b_0)^2$. Here, b_0 is the equilibrium bond length and K_0 is the force constant. The chain rigidity is given by $U(\theta)=\frac{1}{2}K_b(\cos\theta-\cos\theta_0)^2$, in which θ is the angle formed by two adjacent bonds and K_b is the force constant. For the pairwise interaction of polymer segments, we applied the Lennard-Jones- (LJ-) type potential given by $U(r)=4\varepsilon[(\sigma/r)^{12}-(\sigma/r)^6]$ between different segments, except for the interaction between nearest-neighbor or second-nearest-neighbor segments along the main chain. The cutoff distance of the LJ interactions was 3σ.

Simulations were performed for both bulk samples and confined samples. In the case of the bulk samples, we applied the periodic boundary condition. For the confined samples, the noncrystalline boundary wall could be introduced by various methods. One possible method would be an atomistic one in which the wall particles are randomly placed. Although this atomistic method could reveal the detailed microscopic features of the boundary wall, it requires many simulation runs with different wall atom allocations in order to avoid the effect of the specific initial configuration of wall atoms. Hence, we used the flat-wall 10-4 potential given by $U(r)=4\pi\varepsilon\left[\frac{1}{5}(\sigma/r)^{10}-\frac{1}{2}(\sigma/r)^4\right]+C_{\mathrm{offset}}$ within the cutoff distance ($r_{\mathrm{cutoff}}=\sigma, C_{\mathrm{offset}}=1.2\pi\varepsilon$), and $U(r)=0$ outside the cutoff distance [31–33].

In this study, we considered the simple cases in which crystalline polymer chains are confined within a noncrystalline structureless wall. From the viewpoint of strict correspondence to the experiments, in which the crystalline-noncrystalline block copolymers are often used, one could construct a simulation model in which one end of the polymer chain is always attached to the wall boundaries. We thought that this additional condition would make the ordering phenomena more complex to analyze, especially when we compare the results between confined samples and bulk samples. Hence, we started with the condition in which polymers are simply confined with no additional constraint to the chain end, which would be an ideal first step in the study of polymer crystallization under confinement.

The model parameters and simulation results are expressed in dimensionless reduced units, where the segment diameter σ, the energy parameter ε of interaction potential, and the segment mass are all 1.0. The equilibrium bond length b_0 was 0.4, the elastic constant K_0 of the bond springs was 9000, and the equilibrium angle θ_0 was 0. The bending force constant K_b was 1000 or 2000 for the semiflexible chain molecules and 4000 for the semirigid chain molecules. The number of segments per polymer chain was 40, and the number of polymers in the system was 640. The static properties of our polymer model, which were calculated at $T=15$, are shown in Fig. 1. In the case of periodic boundary condition, the initial size of simulation box was 25.0. In the case of cubic domain samples, the initial size of whole simulation box was 27.0 including the depth 1.0 of repulsive walls at both sides. In the case of spherical domain samples, the initial radius of whole simulation sphere was 16.52 including the depth 1.0 of repulsive wall. We have chosen these system sizes so that the polymer segment density in the free region becomes almost identical. The initial states were

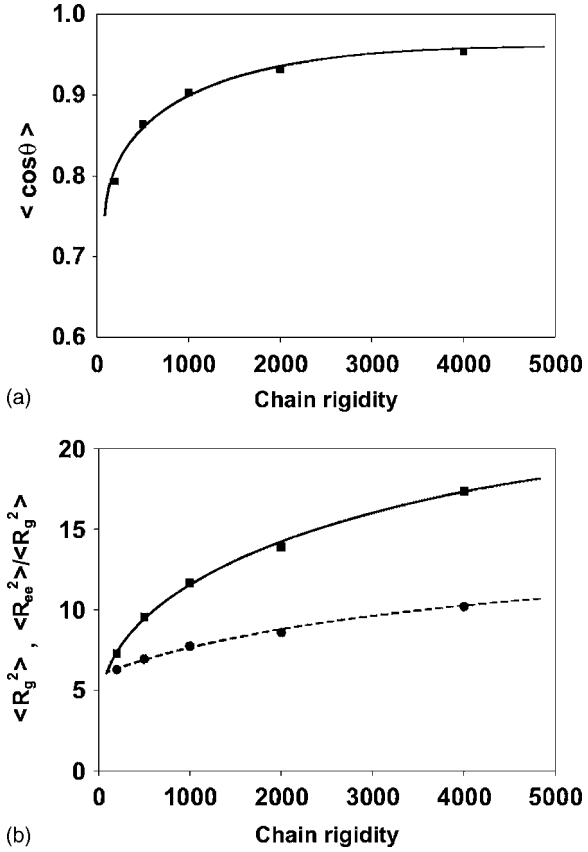

FIG. 1. (a) Relationship between the chain rigidity K_b and the angle correlation of two successive bond vectors. (b) Relationship between the chain rigidity K_b and the radius of gyration R_g. Squares and solid line indicate the $\langle R_g{}^2\rangle$. Circles and dashed line indicate the ratio $\langle R_{ee}{}^2\rangle/\langle R_g{}^2\rangle$, in which R_{ee} is the end to end distance of polymer chains.

prepared by thermally equilibrating using NVT ensemble at a temperature of 15.0, which is well above the melting points of chain molecules. Then the temperature of the system was suddenly cooled by velocity scaling. Since the degree of supercooling might affect the crystallization dynamics, we have chosen the supercooled temperature to be $0.75T_m$, where T_m is the melting point of chain molecules. The relationship between the chain rigidity K_b and the melting point T_m in our model polymer is shown in Fig. 2. In our simulation, the supercooled temperatures were 6.68, 7.50, and 8.32 for the chain molecules with the bending force constants of 1000, 2000, and 4000, respectively. Simulations were carried out using the NPT ensemble for bulk systems, and the NVT or NPT ensemble for confined samples. Temperature and pressure if required were kept constant during the crystallization processes using the Nose-Hoover method. We calculated pressure using the internal pressure. The mass of thermostat was 25 600, the external pressure was 0.007, and its mass parameter was 1.0. The equations of motion are integrated using a forth-order predictor-corrector method with a time step of 0.001. Since the crystallization processes from dense melts are affected by their kinetic paths, which are simply related to the accidental neighboring molecular positions, it may not be sufficient to discuss the evolution curves

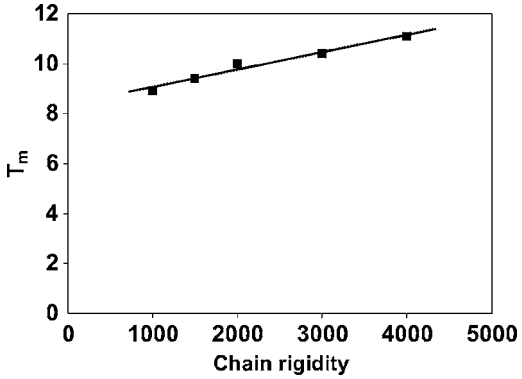

FIG. 2. Relationship between the chain rigidity K_b and the melting temperature.

of only one sample. Therefore, we carried out eight simulation runs from the different initial states and examined the average properties of all simulation runs.

III. RESULTS

A. Crystallization under fixed nanodomain boundary

Snapshots of polymer chains during the crystallization processes are shown in Figs. 3 and 4. Polymers in these figures are the semiflexible chains whose bending force constant is 2000. The results for the cubic domain sample are shown in Fig. 3 and the results for the spherical domain sample are shown in Fig. 4. For the time being, we consider the case in which the structures of the domain interface have not been destroyed during crystallization. This corresponds to the condition in which the glass transition temperature of the noncrystalline polymer around the domain is sufficiently high. In the simulations, the NVT ensemble satisfies this condition. At time 0, chain molecules are randomly allocated within the domain. After temperature cooling, they began to form an ordered structure and eventually became a large crystal region. For a better perspective of the nucleation in the initial time stage, only the molecules that belong to the ordered regions are shown in Figs. 3(d) and 3(e) for the cubic domain sample. In this sample, while most of the chain molecules are in the disordered state at $t=100$, we can observe a small ordered area near the domain interface. Comparison of the ordered region at $t=100$ and $t=200$ reveals that crystal growth proceeded largely around these small nuclei, whereas nucleation continued in the other area. Crystallization behaviors in the spherical domain interface, which are shown in Fig. 4, are generally the same as those in the cubic domain interface.

To analyze the detailed ordering behaviors during polymer crystallization in bulk samples, cubic domain samples or spherical domain samples, we calculated the order parameters of main chain orientation and the crystallinity. Orientation order parameters are given by $\langle 3\cos^2\theta-1\rangle/2$, where θ is the angle formed by two bond vectors of the main chains. The orientation order parameters can be classified into three types by the averaging method. The global order parameter is obtained by averaging over all bond pairs in the entire sys-

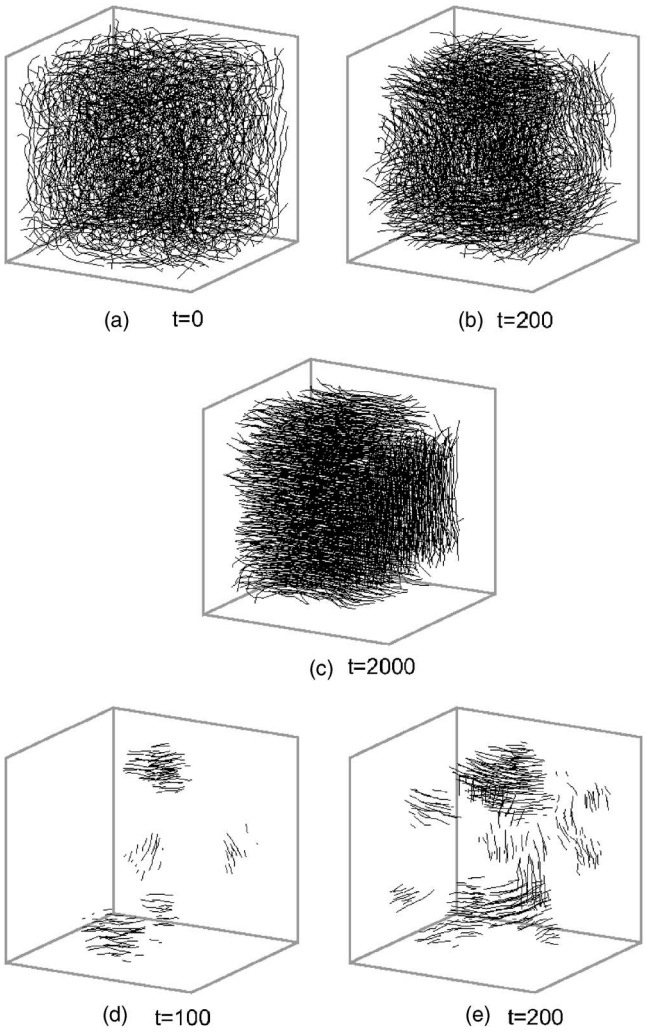

FIG. 3. Snapshots of crystallization processes of semiflexible polymer systems confined to cubic domain. In (a), (b), and (c), whole polymer molecules are shown. In (d) and (e), only the polymers that belong to the crystal regions are shown.

tem region except for bond pairs within the same molecules. The intermolecular local order parameter is calculated only for the pairs of adjacent bonds of different chain molecules. In our simulation, we regard two bonds to be adjacent when the distance between them is less than 1.5. The intramolecular local order parameter is calculated for the pairs of adjacent bonds within the same molecules. These orientation order parameters are useful for analyzing the chain ordering dynamics in various length scales. On the other hand, the entire crystallization behaviors cannot be traced effectively by the global order parameter alone, since its absolute value is strongly influenced by the formation of crystal multidomains. Hence, the crystallinity may be useful in the analysis of the entire behaviors. The crystallinity is the ratio of the number of atoms that belong to the crystals over the number of entire atoms in the system. In our simulation, the crystal domain is defined as the group of segments whose bond vectors are within 1.5 of each other and whose orientation difference is less than 10 degrees. We did not include any group of less than 50 segments among the crystal domains.

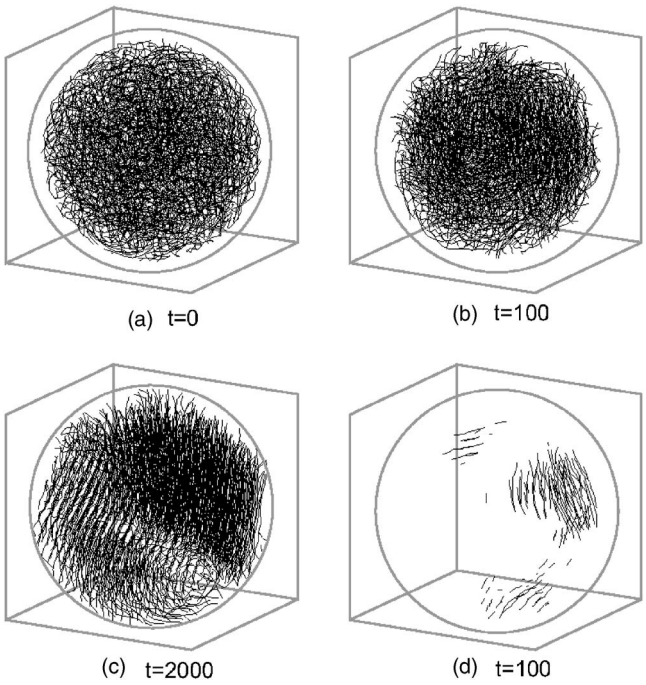

FIG. 4. Snapshots of crystallization processes of semiflexible polymer systems confined to spherical domain. In (a), (b), and (c), whole polymer molecules are shown. In (d), only the polymers that belong to the crystal regions are shown.

In Fig. 5, we show the time evolution of the crystallinity of the semiflexible polymer systems under the bulk condition, cubic domain condition, and spherical domain condition. The values of crystallinity including error bars at the initial and late time stage are summarized in Table I. The bending force constant K_b of these semiflexible chains is 2000. A short induction period is observed just after cooling. Then ordering began to proceed at around a time of 150. The time evolution curves of the crystallinity largely deviate from the sigmoidal function since the build up and saturation curves are not symmetrical in shape. These evolution curves are roughly expressed by the stretched exponential function given by $C=1-\exp(-Kt^n)$, in which the exponent n is around 2. Strictly, there are slight differences between the simulation results and the stretched exponential curve in the

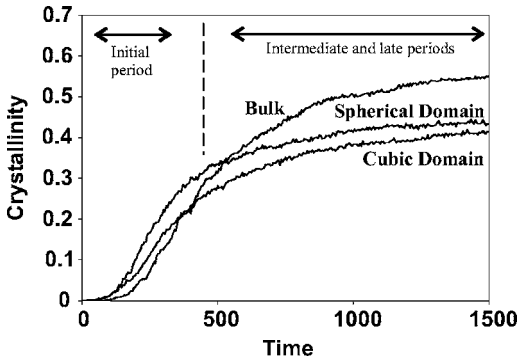

FIG. 5. Time evolution curves of crystallinity of semiflexible polymer systems (K_b=2000) under cubic domain, spherical domain, and bulk conditions.

TABLE I. Crystallinity (%) of semiflexible polymers.

Time	Cubic domain	Spherical domain	Bulk
150	3.74±1.23	5.26±1.83	0.93±0.86
250	11.20±2.34	16.66±5.68	7.11±3.31
2000	42.95±4.97	43.25±1.47	56.69±2.75

intermediate time region and some correction to the fitting equation might be necessary. As shown in this figure, crystallization processes in cubic and spherical domain samples are faster than crystallization processes in bulk samples in the initial time region until about $t=500$. The crystal growth in these confined domain samples gradually slow down, and finally the crystallinity of confined domain samples is surpassed by that of bulk samples in the late time region. To investigate the ordering dynamics in microscopic levels, we show the time evolution of the global order, intermolecular local order, and intramolecular local order in Figs. 6(a)–6(c). As shown in Fig. 6(a), the intramolecular local order parameters grow in almost the same manner in the entire time region for the bulk, cubic domain, and spherical domain samples. This indicates that the persistent length of a polymer chain is mostly governed by the free energy of the local bending of the main chain. The development of the intramolecular configuration has almost finished before the onset of overall crystallization without any large effect of outside chains. On the other hand, in the case of the time evolution curves of the intermolecular local order, there is a marked difference between the confined domain samples and the bulk samples as shown in Fig. 6(b). In the initial time region, the intermolecular local order of the cubic and spherical domain samples are much larger than that of the bulk samples, whereas the difference between the cubic and spherical domain samples is relatively small. This result indicates that there is some enhancement effect on the ordering processes for the confined domain samples in the initial time region. However, in the intermediate or late time region, all three samples show similar order growths, and no significant difference was observed. The behaviors of global orders are slightly different from those of local orders as shown in Fig. 6(c). For all three samples, the growth of order is very slow. Although the global order of the bulk samples showed steady growth in the intermediate or late time region, the growth of the global order of the cubic or spherical domain samples is inhibited. The final global order of confined domain samples reaches only about 1/3 of bulk samples. The global order for the bulk samples is larger than those for the confined domain samples in the whole time region. When the nucleation rate is high, crystal domains with various chain orientations are formed, which sometimes lower the values of the global order parameters.

In Fig. 7, we show the crystallization processes of semiflexible polymer systems, in which the bending force constant K_b of the polymer chain is 1000. This polymer is more flexible than the polymer used in Figs. 5 and 6. As the polymer chains become flexible, the speed of time evolution decreases. The induction period of crystallization was until around $t=250$ for this polymer system. Other than the longer

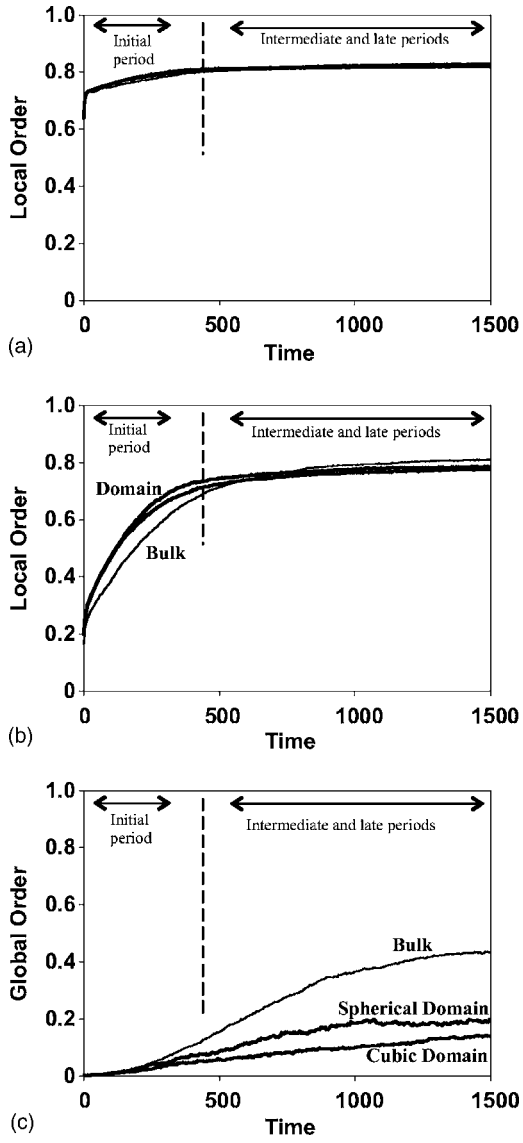

FIG. 6. Time evolution curves of order parameters of semiflexible polymer systems under cubic domain, spherical domain, and bulk conditions. The intramolecular local orientation orders, intermolecular local orientation orders, and global orientation orders correspond to (a), (b), and (c), respectively. The time evolution curves of the bulk samples are plotted in thin lines. The time evolution curves of the cubic and spherical domain samples are plotted in bold lines.

time scale of ordering, the overall behaviors of the crystallinity or the orientation order parameters are generally the same as those of the polymer systems of $K_b=2000$. In the initial time region until $t=700$, the crystallization processes of the confined domain samples are faster than the crystallization processes of the bulk samples, whereas in the intermediate or late time region, the crystallization of the confined domain samples is inhibited to some extent.

Next, we studied the crystallization processes of semirigid polymer systems whose bending force constant K_b was 4000. Time evolution curves of the crystallinity are shown in Fig. 8. The values of crystallinity including error bars at the initial and late time stage are summarized in Table II. In the

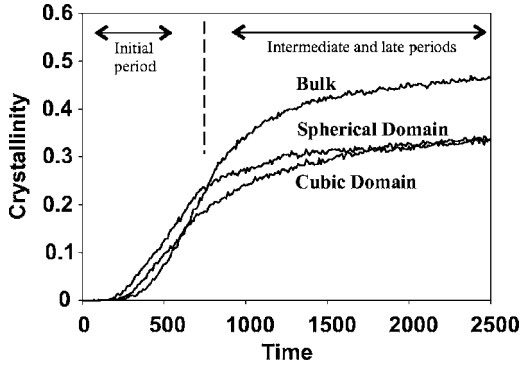

FIG. 7. Time evolution curves of crystallinity of semiflexible polymer systems (K_b=1000) under cubic domain, spherical domain, and bulk conditions. These polymer chains are more flexible than those shown in Fig. 5.

case of these rigid chain molecules, all three samples, which are the cubic domain, spherical domain and bulk samples, show very rapid growth curves. These curves are approximately expressed by a single exponential function given by $1-A\exp(-t/\tau)$. Strictly, there is a slight difference in the intermediate time region. The use of a double exponential curve such as $1-A_1\exp(-t/\tau_1)-A_2\exp(-t/\tau_2)$ gives an exact fitting, in which the longer relaxation component might be related to the slow domain merging process. As shown in this figure, in the case of polymer systems with large chain rigidity, the system becomes unstable below the crystallization temperature and shows a rapid time evolution just after time 0. We compare the crystallization dynamics of the confined domain samples with that of the bulk samples in the initial time region until around t=200. The time evolution curve of the crystallinity of the cubic domain samples is almost the same as that of the bulk samples. In short, the domain interface does not affect the crystallization dynamics for the cubic domain samples in the initial time region. On the other hand, in the case of the spherical domain samples, the value of the crystallinity is larger than that of the bulk samples, which indicates that there is still some kind of enhancement effect in the initial time region. In the intermediate and late periods of crystallization, the growth of the crystallinity of both the cubic and spherical domain samples is

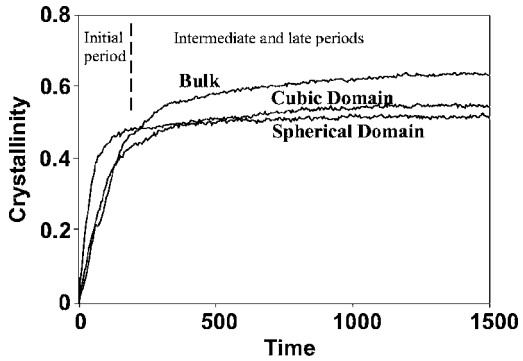

FIG. 8. Time evolution curves of crystallinity of semirigid polymer systems (K_b=4000) under cubic domain, spherical domain, and bulk conditions.

TABLE II. Crystallinity (%) of semirigid polymers.

Time	Cubic domain	Spherical domain	Bulk
20	9.04±3.04	18.70±3.52	6.14±1.43
50	19.55±5.56	34.80±2.08	17.47±3.70
2000	55.33±3.79	52.10±1.10	63.77±2.19

somewhat more inhibited than that of the bulk samples. Thus, in the intermediate and late periods, the crystallization behaviors of semirigid polymer systems have the same tendency as those observed in the semiflexible polymer systems.

The time evolution of the order parameters would give us more detailed information on ordering dynamics. In Figs. 9(a)–9(c), we show the development of the intramolecular

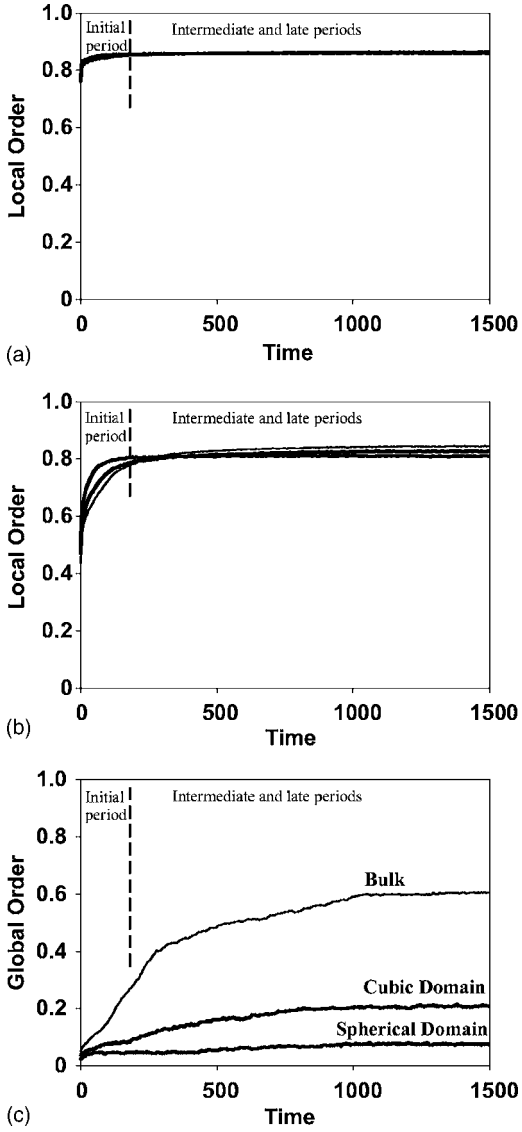

FIG. 9. Time evolution curves of order parameters of semirigid polymer systems under cubic domain, spherical domain, and bulk conditions. The intramolecular local orientation orders, intermolecular local orientation orders, and global orientation orders correspond to (a), (b), and (c), respectively.

local order, intermolecular local order and global order. As shown in Fig. 9(a), the time evolution curves of the intramolecular local order are almost identical. Hence, the intramolecular chain extension processes proceeded irrespective of the existence of the domain boundaries. In the meantime, the behaviors of the intermolecular local order of the confined samples depend on the domain geometry as shown in Fig. 9(b). Whereas the time evolution of the cubic domain samples is almost identical to that of the bulk samples, the growth of the spherical domain samples is faster than that of the bulk samples in the initial period. These behaviors are in good agreement with the results of the crystallinity, in which only the growth of the spherical domain samples is faster than the growth of the cubic domain or bulk samples. In the case of the time evolution of the global order, the growth of the confined domain samples is always smaller than that of the bulk samples. This is the same tendency as that observed in the semiflexible polymer systems. The domain boundary restricts the large orientation relaxation over the whole system, which leads to the formation of multicrystal regions with various orientation directions. As mentioned above, the order formation dynamics of the polymer crystallization in nanodomains has various features due to the enhancement effect of the nucleation processes and the suppression effect of the large-scale chain relaxation processes, which are also closely related to the rigidity of the polymer chains.

To elucidate the nucleation effect in the initial period, we will study the relationship between the orientation order and the depth from the domain surface for both semiflexible and semirigid chain systems. In the calculation of depth profiles, depth is defined as a distance from the nearest walls. In the case of orientation orders, positions that correspond to the center of mass of two bonds are used. In the calculation of crystallinity, we first labeled the polymer segments that belong to the crystal region, and then calculated the ratio of crystalline polymer segments in each depth region. In Fig. 10(a), we show the depth profile of the crystallinity and the intermolecular local order at time 150 for the cubic domain samples of semiflexible polymer systems. The bending force constant the polymer was 2000. The results shown in this figure are the average of eight different samples. As shown in this figure, both the crystallinity and the intermolecular local order take larger values in the shallow depth region near the domain interface. This result supports the assumption described above that the domain interface induces the crystallization in the initial period due to the restriction of freedom of main chain orientation. In Figs. 10(b) and 10(c), we show the time evolution of the depth profiles of the crystallinity and intermolecular local order, respectively. For the best perspective, the vertical axis of the graph of the crystallinity is displayed on a log scale, because the values of crystallinity are very small at the onset of crystallization and cannot be effectively shown in the same chart using a linear scale. As shown in these figures, even when the domain interface consists of the noncrystalline medium, polymer crystallization principally starts near the domain interface region and it gradually progresses towards the inner part of the domain in the case of semiflexible polymer systems. The results of the depth profile of the semiflexible polymer systems confined to the spherical domain are shown in Fig. 11. The ordering

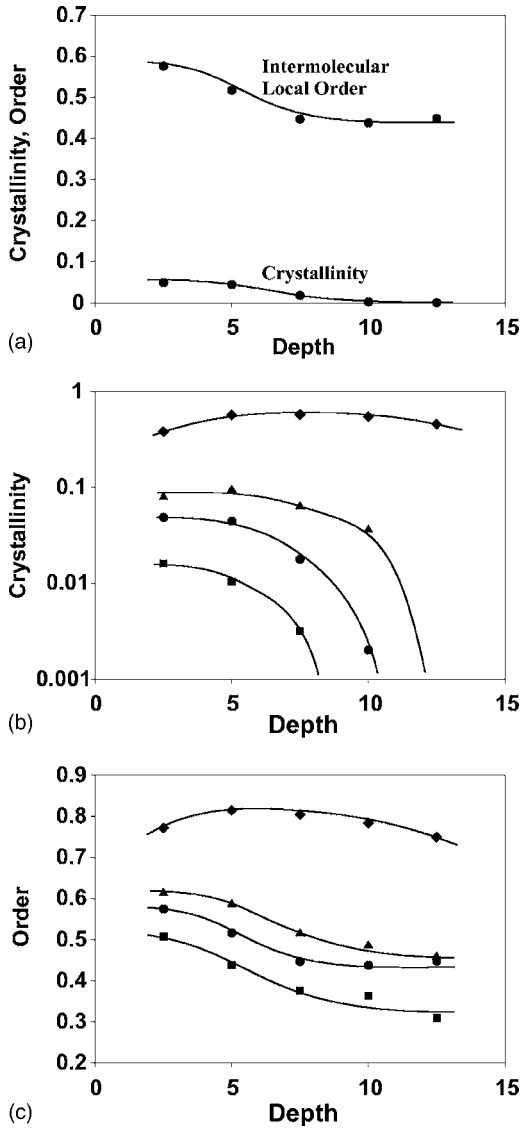

FIG. 10. Depth profiles of intermolecular local order and crystallinity of semiflexible polymer systems (K_b=2000) confined to cubic domain. (a) Profiles at beginning of crystallization (t=150). (b) Temporal change of depth profile of crystallinity. (c) Temporal change of depth profile of intermolecular local order. In (b) and (c), squares, circles, triangles, and diamonds indicate the elapsed time 100, 150, 200, and 2000, respectively.

behaviors in the spherical domain samples are generally the same as those of the cubic domain samples. Therefore, in the case of semiflexible chain systems, the shape of the domain does not play a major role in the initial ordering dynamics, and the existence of the domain interface is the important factor for determining the ordering dynamics.

In Fig. 12, we show the time evolution of the depth profile for semirigid polymer systems confined to the cubic domain. The bending force constant the polymer was 4000. Figure 12(a) shows the development of crystallinity and Fig. 12(b) shows the development of the intermolecular local order. In the case of semirigid polymer systems in the cubic domains, there is no large difference between the region near the domain surface and the internal region. The domain boundary

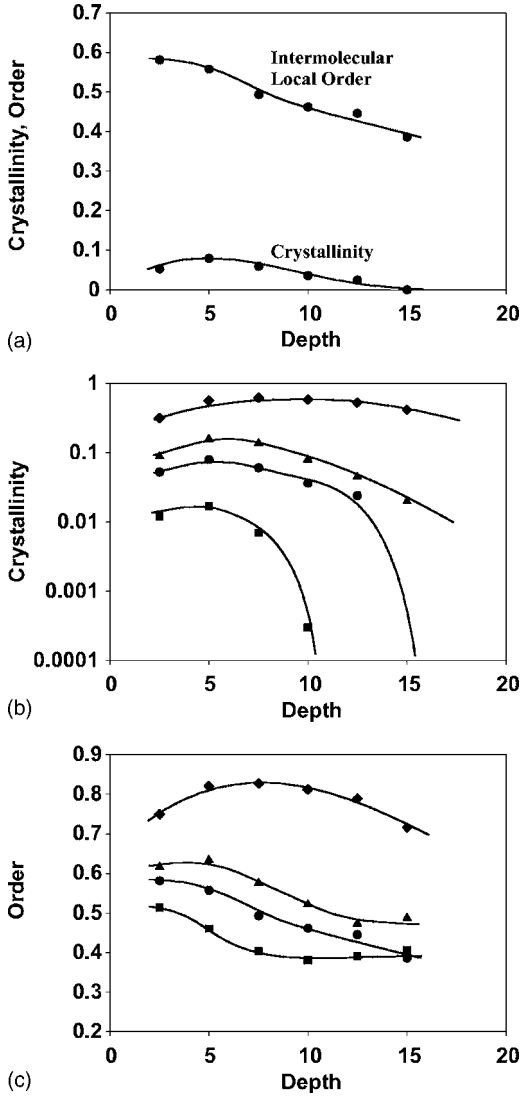

FIG. 11. Depth profiles of intermolecular local order and crystallinity of semiflexible polymer systems confined to spherical domain. (a) Profiles at $t=150$. (b) Temporal change of depth profile of crystallinity. (c) Temporal change of depth profile of intermolecular local order. In (b) and (c), squares, circles, triangles, and diamonds indicate the elapsed time 100, 150, 200, and 2000, respectively.

does not enhance the nucleation in such conditions. These results agree with the behaviors of the crystallinity of the semirigid polymers in that there is no difference between the cubic domain samples and the bulk samples in the initial period. Next, we show the time evolution of the depth profile for the semirigid polymer systems confined to the spherical domains in Fig. 13. Unlike the results in Fig. 12, the depth profile of spherical domain samples shows that the region near the domain surface has slightly higher levels of crystallinity and intermolecular local order than the internal domain region. Hence, in the case of spherical domains, there still remains some enhancement effect of crystallization in the initial period, which leads to the acceleration of the growth of the crystallinity of the entire polymer system.

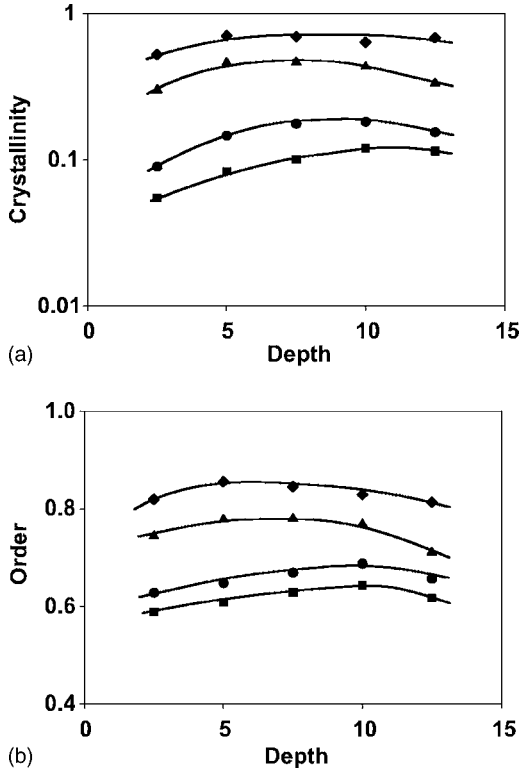

FIG. 12. Depth profiles of crystallinity (a) and intermolecular local order (b) of semirigid polymer systems ($K_b=4000$) confined to cubic domain. Squares, circles, triangles, and diamonds indicate the elapsed time 10, 20, 100, and 2000, respectively.

B. Crystallization under isotropic deformation of nanodomain

In the previous section, we assume that the glass transition temperature of the noncrystalline medium, which surrounds the domain boundary, is sufficiently high so that the domain structure is not destroyed during crystallization. In general, when the noncrystalline polymer block is glassy, polymers crystallize with the nanodomain structure unchanged, which justifies the simulation assumptions that the domain boundary is fixed. However, the structure of the surrounding amorphous medium may not always be strong. It would be important to consider the case in which the domain structure can be destroyed or transformed by the crystallization within the domain. In fact, when the structure of the noncrystalline part and the segregation force are weak, the nanoscale domain structure is completely destroyed during crystallization and a new crystal structure is formed. Of course, this is an extreme case, and it would be better modeled as a usual melt crystallization process with a specific polymer interaction and an initial polymer allocation, rather than the modified model of the polymer crystallization confined to domains.

In this section, we will examine the situations in which the isotropic volume change of the crystalline polymer domain is allowed, although the drastic destruction of the domain structure is not considered. In this case, the degree of easiness of domain deformation, which corresponds to the mass parameter of the pressure in the NPT ensemble, is an important factor for ordering dynamics. In this study, we will

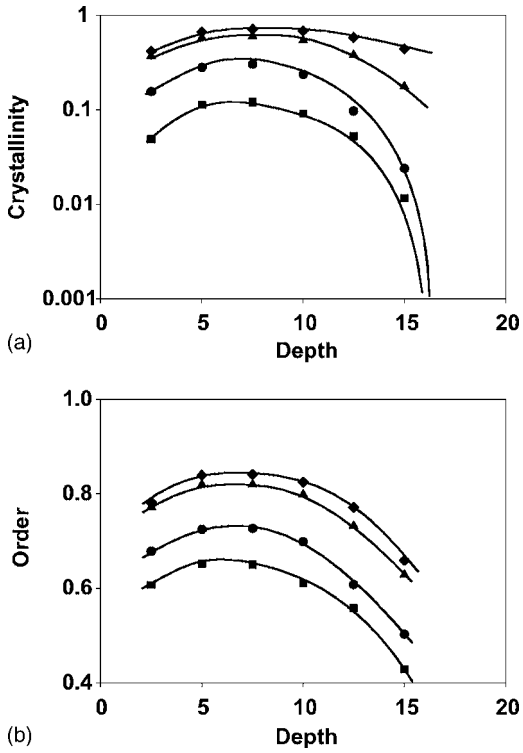

FIG. 13. Depth profiles of crystallinity (a) and intermolecular local order (b) of semirigid polymer systems confined to spherical domain. Squares, circles, triangles, and diamonds indicate the elapsed time 5, 20, 100, and 2000, respectively.

consider the case in which the motion of the domain interface is very easy as in the case of the liquid polymer melt in the bulk. This condition was chosen as the case that was completely opposite to that of the fixed volume condition reported in the previous section. In actual cases, the ordering behaviors would be in the middle of those observed in these two conditions depending on the ease of domain deformation. In this simulation, we kept the pressure within the domain equal to atmospheric pressure and the mass parameter of the pressure in the NPT ensemble was 1.0, which was the same value as in the bulk polymer systems. This choice would also be suitable from the viewpoint of a direct comparison with the bulk systems. We only considered the isotropic deformation, where the symmetry of domain shape was preserved. In simulations, the existence of movable repulsive boundary walls makes the final system volume more compact than that of periodic bulk samples. The volume reduction of the final crystal configuration with respect to the initial configuration of the confined domain samples were slightly more than 30%, while those of periodic bulk samples were about 20%. Although it might be possible to choose appropriate different pressure parameters to adjust the volume reduction rate, we used the same pressure parameters as bulk samples for direct comparison, since our major purpose was the verification of universality of simulation results obtained at the previous section.

First, we show the crystallization behaviors of the semiflexible polymer chain systems, in which the bending force constant is 2000. The time evolution of the crystallinity and

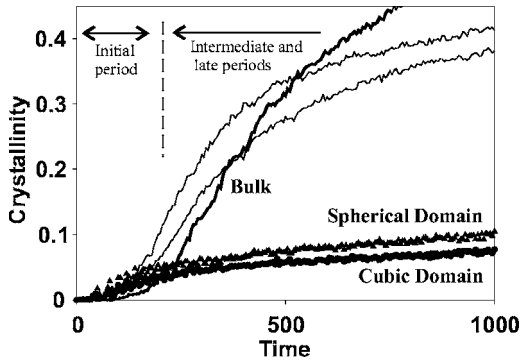

FIG. 14. Time evolution curves of crystallinity of semiflexible polymer systems (K_b=2000) at cubic domain and spherical domain. Deformation of the domain boundary is allowed here. Circles and triangles indicate the results of the cubic domain and spherical domain, respectively. For comparison, the time evolution curve of the bulk system and the time evolution curves of the confined domain system with the fixed domain boundary are plotted in thin lines.

that of the intermolecular local order are shown in Figs. 14 and 15, respectively. For comparison, the simulation results of the confined polymer systems in which the domain interface did not move are shown as thin lines. As shown in Fig. 14, when the domain interface is very easy to deform, the crystalline regions are often destroyed by the domain boundary and the growth of the crystallinity is considerably inhibited especially in the late period. However, in the initial period, the growth of the crystallinity of the confined domain samples is faster than that of the bulk systems. In this sense, even when the domain boundary can be freely transformed, these ordering behaviors are explained by the same framework of the ordering dynamics of the confined domain polymers.

Next, we show the results for crystallization behaviors under domain deformation for the semirigid polymers in Figs. 16 and 17. The bending force constant of the semirigid polymer chain is 4000. Although some oscillations are observed in growth curves, this is not essential. In the case of the rigid chain systems, the initial shock of the volume change due to instant temperature cooling is not effectively absorbed by the relaxation inside polymer molecules, and the

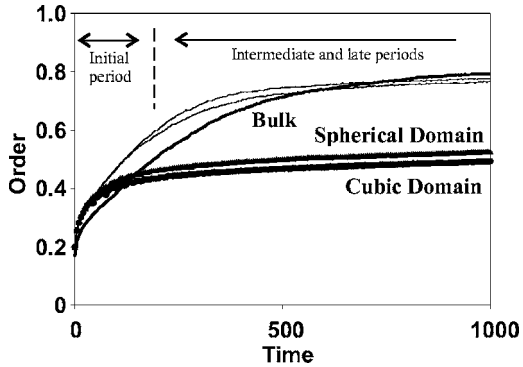

FIG. 15. Time evolution curves of intermolecular local order of semiflexible polymer systems at cubic domain and spherical domain. Deformation of the domain boundary is allowed here. The symbols are the same as those in Fig. 14.

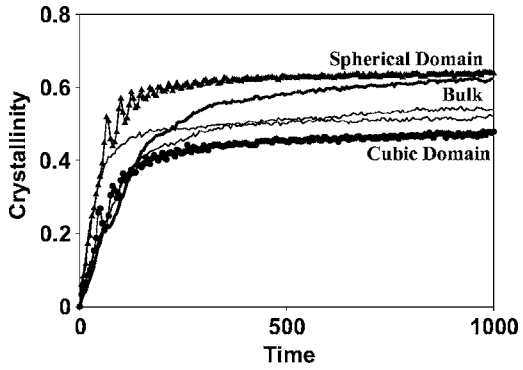

FIG. 16. Time evolution curves of crystallinity of semirigid polymer systems (K_b=4000) at cubic domain and spherical domain. Deformation of the domain boundary is allowed here. The symbols are the same as those in Fig. 14.

crystal structure of the polymer systems becomes very sensitive to the change in internal pressure and volume in the initial period. However, in actual cases, these oscillations do not occur since the domain wall is not so movable as liquid polymer melt and there is a limit in the temperature cooling rate. In addition, in the case of real systems, there are many domains in the system. The size of these domains and the strength of the surrounding domain wall cannot be the same for all domains since there will always be some variations around average values. If we prepare simulation samples with various domain sizes and various mobilities for surrounding domain walls, the oscillation periods of each domain will differ and the average behaviors will become smooth. Hence, in the following, we will consider the ordering behaviors on a time scale longer than this period. As shown in Fig. 16, in the case of the semirigid polymer systems, the crystal growth is not markedly suppressed in the intermediate or late period. In the cubic domain samples, the time evolution curves of crystallinity are almost the same between fixed and movable domain boundary conditions. In particular, it is remarkable that the degree of the crystallization of the spherical domain samples is larger than that of the bulk samples even in the late time region. Thus, the effect of the volume change of the polymer domain has various features depending on whether the polymer chain is semiflexible or semirigid. In the case of semirigid polymer systems, a solid crystal structure is formed in the initial period, which keeps the crystal structure firmly under the deformation to some extent.

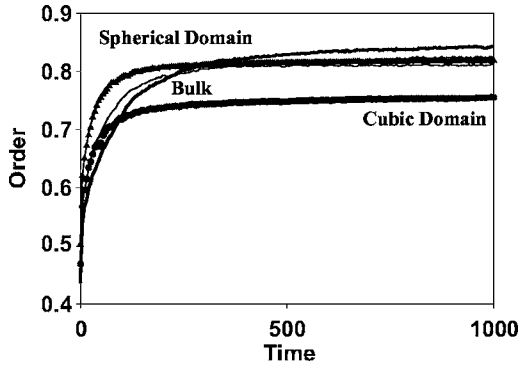

FIG. 17. Time evolution curves of intermolecular local order of semirigid polymer systems at cubic domain and spherical domain. Deformation of the domain boundary is allowed here. The symbols are the same as those in Fig. 14.

IV. DISCUSSION

As mentioned in the simulation results, the crystallization dynamics of the polymer systems in the nanodomains confined to the noncrystalline medium shows features that differ from those of the crystallization dynamics of the bulk polymers. In addition, the effect of the domain interface varies with the time region and the rigidity of polymer chains. In the case of semiflexible polymer systems, in which the intermolecular interaction is not so strong and the nucleation from thermodynamically metastable states is dominant, the confined domain samples show faster crystallization in the initial period. Even when the domain interface consists of noncrystalline molecules and there is no substrate to induce the crystalline layer, restriction of the orientation of polymer chains may enhance the intermolecular ordering processes. Although there is some difference in the time evolution of crystallinity owing to the shape of domains, domain shape has a minor effect, and the existence of the domain interface is a critical factor. In the intermediate or late period of crystallization, the existence of the domain interface becomes an obstacle for the global orientation relaxation of the polymer chains. The crystallinity in the late period is smaller than the crystallinity obtained from the bulk polymer systems by the ideal homogeneous nucleation processes.

On the other hand, the behaviors of semirigid polymer systems confined to nanodomains are different from those of semiflexible polymers. In the case of semirigid polymer systems, where the effective intermolecular orientation interaction is strong, the inductive effect of the nucleation due to the restriction of the degree of the chain orientation by the domain interface cannot efficiently work, since the rapid spontaneous nucleation process inside the polymer melts becomes dominant. This is especially pronounced in the samples of cubic domain shape. In the case of semirigid polymer systems, ordering dynamics is affected by the domain shape. The spherical domain samples show faster crystallization than the cubic domain or bulk samples in the initial period. The reason for this behavior is not necessarily clear, but we consider the following. In general, when the system volume is identical, the surface area of a sphere is 20% smaller than that of a cube. However, in the case of the cubic domain systems, the areas near the corners have a disadvantage in ordering carried out by the parallel orientation packing of polymer chains. Hence, from the point of view of the effective surface area in polymer crystallization, the spherical domain interface becomes superior to the cubic domain interface, since the entire surface area contributes equally to induce nucleation. Therefore, in the case of the spherical domain system, the inductive effect of the nucleation brought about by the domain interface still prevails, which leads to the faster crystallization dynamics in the initial period.

Next, we will consider the relationship between experimental results. In the case of experimental observations,

there are many nanodomains within the observation area, and the overall dynamics of these many domains are obtained. In contrast, the simulation system contains only one domain in the simulation box. However, in the case of our simulations, we took many ensemble averages, which led to the same simulation results for a large number of domains. Here, note that most of the experiments on the polymer crystallization in nanodomains focused on static properties, such as crystal structures, and experiments on the ordering kinetics are very limited. Therefore, it is not always certain whether the observed kinetics are the universal behaviors for all confined polymer systems or the peculiar behaviors only for specific kinds of polymer systems.

In general, under moderate supercooling conditions, the experimentally observed crystal growth of the polymer system in the bulk is often expressed by the stretched exponential functions. This is because a thermodynamically unstable condition is required in order to realize the exponential-type rapid crystal growth in the bulk polymer systems. Such a condition may be realized when the extended polymer chains with a certain degree of persistent length exist at high density in the system. There are some reports that crystal growth of the exponential form was observed under certain molecular or domain interface conditions, whereas the crystal growth under other conditions was of the usual stretched exponential form [1–3]. This behavior shows the same tendency as that observed at our simulation, in which the existence of the noncrystalline domain interface accelerates crystallization in the initial period. If the nucleation in the initial period increases to some extent, the system would approach the exponential-type growth from unstable states. Thus, the simulation results provide qualitative explanations to some extent. However, in this simulation study, no considerable change in the shape of the growth curves could be observed, such as from the stretched exponential curves to the exponential curves, between the bulk samples and the confined domain samples. Of course, there remain some possibilities that the function form of the growth curves of the crystallization might be greatly changed between the bulk and the confined samples by an appropriate choice of simulation conditions, such as molecular parameters, degree of supercooling or system size. However, we think that additional conditions would be necessary in order to change the function type of the growth curve significantly. For example, in this simulation study, we used the free polymer chains inside the domain boundary rather than the block copolymers whose noncrystalline unit constitutes the domain boundary. This is because in order to understand the basic physics of the crystallization dynamics induced by the confinement, a simplified model is necessary for the comparison with the bulk polymer systems. In the case of block copolymers, one end segment of a crystalline polymer chain, which corresponds to the junction of a crystalline-noncrystalline block polymer, exists in the region near the domain interface at high probability. Under these constraints, it is possible that the time evolution curves of the semiflexible polymer systems confined to domains might change significantly from those of the bulk, since the initial orientation of the polymer chain could become easier.

In general, polymer crystallization confined to nanodomains is a complicated process, in which various factors are concerned. Systematic investigation of the ordering mechanism by changing a single factor has not been an easy experimental task. For the elucidation of the fundamental ordering mechanism, it is important to investigate each factor independently. Our simulation results revealed the role of confinement by a noncrystalline medium with other external conditions being kept constant. Thus, the coarse-grained molecular dynamics simulation is an effective tool for this purpose. In our present study, some factors are not considered and their roles remain unresolved. These factors are the geometrical constraint of block copolymer cases, the molecular weight of the polymer chains, the size of the domains, and anisotropic deformation of domain walls. These would be interesting research subjects. We believe that our simulation study, which considers the effect of confinement by a noncrystalline medium, would be a useful first step towards understanding polymer crystallization in nanodomains.

V. CONCLUSION

In summary, we have investigated the ordering dynamics of polymer crystallization, in which the polymers are confined to small nanodomains surrounded by a noncrystalline amorphous medium. We prepared two differently shaped domain structures, namely, the cubic domain and spherical domain structures, and compared the crystallization dynamics with that of bulk polymers. We found that existence of a noncrystalline domain interface has two opposite effects on the crystallization processes. In the case of semiflexible polymer systems, it accelerates the ordering processes in the initial period. When the boundary interface is of noncrystalline structure, there are no adsorption and realignment processes on the surface. However, restriction of the freedom of the orientation order near the domain surface induces the nucleation processes, which leads to the acceleration of crystallization processes in the initial period. On the other hand, in the intermediate or late period of crystallization, the crystal growth of the confined domain samples is suppressed. In the late period, the existence of the domain interface interferes with the relaxation of the orientation order of the polymer chain on a larger scale, which results in smaller values of crystallinity than those of bulk samples. The crystallization dynamics of the confined domain samples is also affected by the rigidity of polymer chains and the strength of the domain boundary. In the case of semirigid polymer systems, there are no large differences in the initial growth of the crystallinity and the intermolecular local order between the cubic domain samples and the bulk samples. When the rigidity of the polymer chain is large, the acceleration effect of the nucleation induced by the domain interface is hidden by the spontaneous homogeneous nucleation inside polymer melts, and the effect of the domain interface in the initial period becomes less important. The strength of the domain wall structure also has two opposite effects, which are closely related to the rigidity of polymer chains. In the case of semiflexible polymer systems, the deformation of the domain wall suppresses crystallization growth largely in the intermediate or late period. In contrast, in the case of semirigid polymer systems,

the deformation of the domain wall does not have a large effect for the cubic domain samples, and it even accelerates the crystallization for the spherical domain samples. Thus, our simulation results revealed that the confinement by the noncrystalline medium does not have a simple effect on the polymer crystallization dynamics, but has various conflicting effects combined with the time stage, the rigidity of polymer chains, and the strength of the surrounding domain interface.

[1] Y. L. Loo, R. A. Register, and A. J. Ryan, Phys. Rev. Lett. **84**, 4120 (2000).
[2] Y. L. Loo, R. A. Register, A. J. Ryan, and G. T. Dee, Macromolecules **34**, 8968 (2001).
[3] Y. L. Loo, R. A. Register, and A. J. Ryan, Macromolecules **35**, 2365 (2002).
[4] S. Nojima, M. Toei, S. Hara, S. Tanimoto, and S. Sasaki, Polymer **43**, 4087 (2002).
[5] A. Rottele, T. Thurn-Albrecht, J. U. Sommer, and G. Reiter, Macromolecules **36**, 1257 (2003).
[6] Q. Guo, R. Thomann, W. Gronski, R. Staneva, R. Ivanova, and B. Stuhn, Macromolecules **36**, 3635 (2003).
[7] L. Sun, L. Zhu, Q. Ge, R. P. Quirk, C. C. Xue, S. Z. D. Cheng, B. S. Hisao, C. A. Avila-Orta, I. Sics, and M. E. Cantino, Polymer **45**, 2931 (2004).
[8] R. M. Ho, Y. W. Chiang, C. C. Lin, and B. H. Huang, Macromolecules **38**, 4769 (2005).
[9] T. Miura, R. Kishi, M. Mikami, and Y. Tanabe, Phys. Rev. E **63**, 061807 (2001).
[10] T. Miura, R. Kishi, and M. Mikami, J. Chem. Phys. **119**, 6354 (2003).
[11] T. Miura, R. Kishi, A. Kaito, and M. Mikami, Mol. Simul. **30**, 987 (2004).
[12] T. Yamamoto, Adv. Polym. Sci. **191**, 37 (2005).
[13] M. Muthukumar, Adv. Polym. Sci. **191**, 241 (2005).
[14] K. Esselink, P. A. J. Hilbers, and B. W. H. van Beest, J. Chem. Phys. **101**, 9033 (1994).
[15] T. Shimizu and T. Yamamoto, J. Chem. Phys. **113**, 3351 (2000).
[16] T. Yamamoto, J. Chem. Phys. **115**, 8675 (2001).
[17] A. Koyama, T. Yamamoto, K. Fukao, and Y. Miyamoto, Phys. Rev. E **65**, 050801(R) (2002).
[18] H. Meyer and F. Muller-Plathe, J. Chem. Phys. **115**, 7807 (2001).
[19] H. Meyer and F. Muller-Plathe, Macromolecules **35**, 1241 (2002).
[20] R. H. Gee and L. E. Fried, J. Chem. Phys. **118**, 3827 (2003).
[21] H. Meyer and J. Baschnagel, Eur. Phys. J. E **12**, 147 (2003).
[22] M. J. Ko, N. Waheed, M. S. Lavine, and G. C. Rutledge, J. Chem. Phys. **121**, 2823 (2004).
[23] A. Marbeuf and R. Brown, J. Chem. Phys. **124**, 054901 (2006).
[24] M. Wang, W. Hu, Y. Ma, and Y. Q. Ma, J. Chem. Phys. **124**, 244901 (2006).
[25] F. Varnik, J. Baschnagel, and K. Binder, Phys. Rev. E **65**, 021507 (2002).
[26] F. Varnik, J. Baschnagel, K. Binder, and M. Mareschal, Eur. Phys. J. E **12**, 167 (2003).
[27] J. Baschnagel and F. Varnik, J. Phys.: Condens. Matter **17**, R851 (2005).
[28] J. H. Jang and W. L. Mattice, Macromolecules **33**, 1467 (2000).
[29] J. Chang, J. Han, L. Yang, R. L. Jaffe, and D. Y. Yoon, J. Chem. Phys. **115**, 2831 (2001).
[30] V. Kuppa and E. Manias, J. Chem. Phys. **118**, 3421 (2003).
[31] S. A. Somers and H. T. Davis, J. Chem. Phys. **96**, 5389 (1992).
[32] G. S. Grest, J. Chem. Phys. **105**, 5532 (1996).
[33] A. Jabbarzadeh, J. D. Atkinson, and R. I. Tanner, J. Chem. Phys. **110**, 2612 (1999).